A thermogenic fat-epithelium cell axis regulates intestinal disease tolerance

Kevin Man[a,b,1], Christopher Bowman[c], Kristina N. Braverman[d], Veronica Escalante[e], Yuan Tian[f], Jordan E. Bisanz[e], Kirthana Ganeshan[a], Biao Wang[a,g], Andrew Patterson[f], James R. Bayrer[d], Peter J. Turnbaugh[e], and Ajay Chawla[a,g,h,1]

[a]Cardiovascular Research Institute, University of California, San Francisco, CA 94143-0795; [b]Department of Medical Biology, University of Melbourne, Parkville, VIC 3010, Australia; [c]Department of Pathology, University of California, San Francisco, CA 94143-0795; [d]Department of Pediatrics, Division of Gastroenterology, University of California, San Francisco, CA 94143; [e]Department of Microbiology and Immunology, University of California, San Francisco, CA 94143-0795; [f]Department of Veterinary and Biomedical Sciences, Penn State College of Agricultural Sciences, University Park, PA 16802; [g]Department of Physiology, University of California, San Francisco, CA 94143-0795; and [h]Department of Medicine, University of California, San Francisco, CA 94143-0795

Edited by Miguel P. Soares, Instituto Gulbenkian de Ciência, Oeiras, Portugal, and accepted by Editorial Board Member Robert L. Coffman October 30, 2020 (received for review June 10, 2020)

Disease tolerance, the capacity of tissues to withstand damage caused by a stimulus without a decline in host fitness, varies across tissues, environmental conditions, and physiologic states. While disease tolerance is a known strategy of host defense, its role in noninfectious diseases has been understudied. Here, we provide evidence that a thermogenic fat–epithelial cell axis regulates intestinal disease tolerance during experimental colitis. We find that intestinal disease tolerance is a metabolically expensive trait, whose expression is restricted to thermoneutral mice and is not transferable by the microbiota. Instead, disease tolerance is dependent on the adrenergic state of thermogenic adipocytes, which indirectly regulate tolerogenic responses in intestinal epithelial cells. Our work has identified an unexpected mechanism that controls intestinal disease tolerance with implications for colitogenic diseases.

tissue tolerance | resilience | immunity | cancer | metabolism

Resistance and disease tolerance are two distinct strategies a host can use to mitigate the negative impact of disease on tissue function and host fitness (1, 2). For example, during pathogenic infections, the detection and elimination of pathogens is mediated by resistance, whereas disease tolerance minimizes the negative impact of pathogens on host fitness without affecting pathogen burden. Although disease tolerance is a well-appreciated strategy of host defense against pathogens in both the plant and animal kingdoms (3–5), its importance in noninfectious diseases is largely unknown (1, 6).

Recent studies have demonstrated that metabolic adaptations mediate disease tolerance during viral, bacterial, and parasitic infections (7–12). These findings suggest that disease tolerance programs are metabolically expensive and compete for energy with other tissue maintenance programs. Because homeothermy, the stable maintenance of core temperature, is a major energy consuming program in mammals (13), we postulated that it might energetically compete with disease tolerance programs to limit their expression in noninfectious diseases. We tested this hypothesis using murine models of colitis because the high regenerative capacity of the intestinal epithelium has been postulated to increase its intrinsic tolerance capacity (1).

Results and Discussion

Thermoneutral Mice Exhibit Intestinal Disease Tolerance. Our experimental design consisted of breeding and housing mice at two different ambient temperatures (T_a) and challenging them with dextran-sodium sulfate (DSS)-induced colitis. Mice were housed at the normal vivarium temperature of 22 °C, a subthermoneutral environment that activates adaptive thermogenesis in brown and beige adipocytes for maintenance of core temperature, and thermoneutrality (T_a = 30 °C), which minimizes reliance on adaptive thermogenesis (13). Using this experimental design, we observed that both male and female C57BL/6J mice housed at thermoneutrality were more tolerant to DSS-induced colitis. For example, compared to mice housed at subthermoneutrality (T_a = 22 °C), thermoneutral mice lost less body mass (Fig. 1 *A* and *B*), which was associated with decreased colon shortening (Fig. 1*C* and *SI Appendix*, Fig. S1 *A–C*) and histopathological evidence of colitis (Fig. 1 *D* and *E* and *SI Appendix*, Fig. S1 *D* and *E*). To determine whether higher host fitness at thermoneutrality resulted from a difference in disease tolerance, we generated reaction norm plots, a measure of how a given genotype responds to a range of environmental conditions (5), using colon shortening as a marker of host fitness and lipocalin-2 as a biomarker of intestinal damage (14). We found that, while plasma levels of lipocalin-2 were similar between mice housed at 22 °C and 30 °C (Fig. 1*F* and *SI Appendix*, Fig. S1*F*), thermoneutral mice had a lower slope on the reaction norm plots (Fig. 1*G* and *SI Appendix*, Fig. S1*G*), suggesting improvement in host fitness stems from higher disease tolerance. In support of this hypothesis, bacterial burden in spleen, liver, and gonadal white adipose tissue was similar in both groups of mice (*SI Appendix*, Fig. S1 *H* and *I*). Thermoneutral mice also exhibited less wasting (higher

Significance

Disease tolerance is a host defense strategy that protects tissues from damage caused by pathogens or the immune system. While the importance of disease tolerance is well established in pathogenic infections, its role in tissue protection in noninfectious diseases remains less well understood. Here, we provide a framework for investigating the mechanisms of disease tolerance in experimental models of colitis. We find that the program of disease tolerance is preferentially expressed in thermoneutral mice, which protects them from injury-induced colitis and inflammation-induced colon cancer. The expression of intestinal disease tolerance is mediated by an unexpected cross-talk between thermogenic adipocytes and intestinal epithelial cells, suggesting that disease tolerance programs are metabolically expensive and dependent on the energetic state of the host.

Author contributions: K.M., K.N.B., V.E., K.G., A.P., J.R.B., P.J.T., and A.C. designed research; K.M., C.B., K.N.B., V.E., Y.T., J.E.B., A.P., and J.R.B. performed research; K.M., C.B., K.N.B., V.E., Y.T., J.E.B., B.W., A.P., J.R.B., P.J.T., and A.C. contributed new reagents/analytic tools; K.M., C.B., K.N.B., V.E., Y.T., J.E.B., A.P., J.R.B., P.J.T., and A.C. analyzed data; and K.M., J.E.B., P.J.T., and A.C. wrote the paper.

The authors declare no competing interest.

This article is a PNAS Direct Submission. M.P.S. is a guest editor invited by the Editorial Board.

Published under the PNAS license.

[1]To whom correspondence may be addressed. Email: kevin.man.ucsf@gmail.com or ajay.chawla@merck.com.

This article contains supporting information online at https://www.pnas.org/lookup/suppl/doi:10.1073/pnas.2012003117/-/DCSupplemental.

First published November 30, 2020.

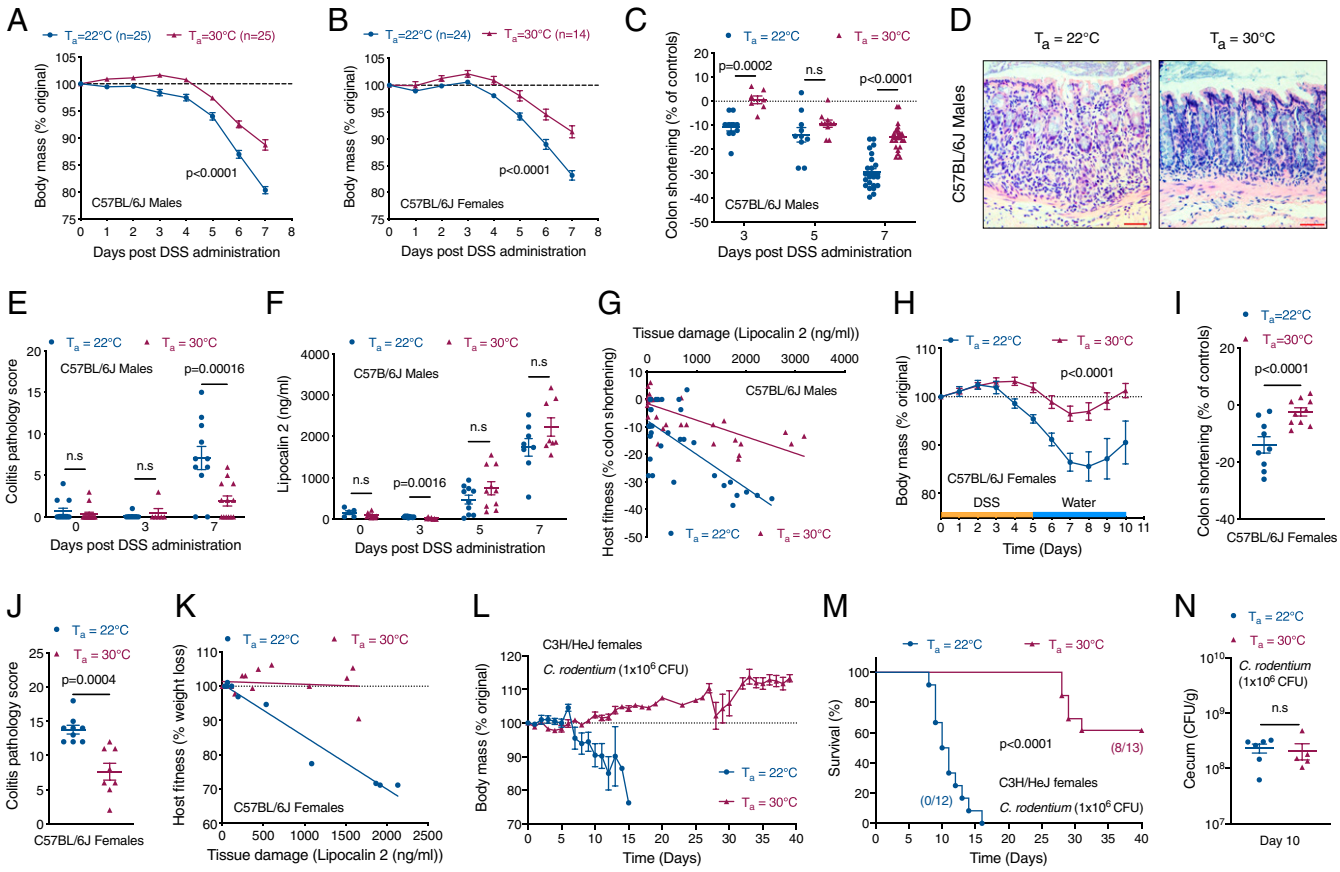

Fig. 1. Thermoneutral mice exhibit intestinal disease tolerance. (*A–G*) To induce colitis, C57BL/6J mice housed at T_a = 22 °C or T_a = 30 °C were administered 4% DSS in drinking water for 7 d. (*A–C*) Body mass of male (*A*) and female (*B*) C57BL/6J treated mice (n = 25 per temperature for males and n = 14 to 25 per temperature for females; data pooled from n = 4 independent experiments and analyzed by two-way ANOVA) and colon shortening in C57BL/6J male treated mice (n = 7 to 25 per time point and temperature; data pooled from n = 4 independent experiments and analyzed by Student's t test). (*D*) Representative pictures of hematoxylin and eosin (H&E)-stained sections of colon. (Scale bar: 100 μM.) (*E*) Colitis pathology score in C57BL/6J male treated mice (n = 6 to 15 per time point and temperature; data pooled from n = 3 independent experiments and analyzed by Student's t test). (*F*) Plasma levels of lipocalin 2, a tissue damage marker, in C57BL/6J male mice administered DSS and housed at T_a = 22 °C or T_a = 30 °C (n = 5 to 11 per time point and temperature; data pooled from n = 3 independent experiments and analyzed by Student's t test). (*G*) Reaction norm plots of host fitness (colon shortening) and tissue damage (lipocalin 2) during DSS-induced colitis in C57BL/6J male mice housed at T_a = 22 °C or T_a = 30 °C (n = 35 per temperature; data pooled from n = 4 independent experiments). (*H–K*) To monitor tissue regeneration, mice were administered 4% DSS in drinking water for 5 d followed by recovery over the next 5 d. Body mass (*H*; analyzed by two-way ANOVA), colon shortening (*I*), and colitis pathology score (*J*) of C57BL/6J female treated mice (n = 9 to 10 per temperature; data pooled from n = 2 independent experiments and analyzed by Student's t test). (*K*) Reaction norm plots of host fitness (weight loss) and tissue damage (lipocalin 2) during DSS-induced colitis and recovery in female C57BL/6J mice housed at T_a = 22 °C or T_a = 30 °C (n = 9 to 10 per temperature; data pooled from n = 2 independent experiments). (*L–N*) C3H/HeJ female mice housed at T_a = 22 °C or T_a = 30 °C were orally infected with *C. rodentium* [1×10^6 colony-forming units (CFUs)]. Body mass (*L*) and survival (*M*) was monitored over 40 d (n = 12 to 13 per temperature; data pooled from n = 2 independent experiments; survival curves analyzed by log-rank Mantel–Cox test). (*N*) Bacterial CFUs in cecum were quantified on day 10 (n = 5 to 6 per temperature; data representative of n = 2 independent experiments and analyzed by Student's t test). Data are presented as mean ± SEM.

mass of white adipose depots) and splenomegaly (*SI Appendix*, Fig. S1 *J–M*), findings that are consistent with their higher disease tolerance.

To rule out alternative explanations for the observed differences in host fitness, we quantified biomarkers of tissue damage and the systemic inflammatory response during DSS-induced colitis. We found that transaminases and blood urea nitrogen, biomarkers of liver and kidney damage, respectively, were not significantly different between the two groups (*SI Appendix*, Fig. S2 *A–D*). Furthermore, plasma levels of cytokines (IL-6, IL-10, MCP-1, IL-12p70, IFNγ, and TNF) and the acute phase reactant serum amyloid A1 were also comparable (*SI Appendix*, Fig. S2 *E–L*). The higher tolerance of thermoneutral mice during colitis was also independent of water consumption and energetic trade-offs (*SI Appendix*, Fig. S3 *A* and *B*); the latter was assessed by monitoring core temperature by telemetry (*SI Appendix*, Fig. S3 *C* and *D*). A modest reduction in core temperature (~1.5 to 2 °C) on days 5 to 7 was observed in mice treated with DSS at 22 °C (*SI Appendix*, Fig. S3*C*), which likely resulted from a decrease in locomotor activity (*SI Appendix*, Fig. S3 *E* and *F*), findings consistent with increased tissue damage and lethargy in mice housed at 22 °C.

We used two additional models to confirm presence of increased intestinal disease tolerance in thermoneutral mice. First, we employed a regenerative paradigm in which mice were treated with DSS-containing water for 5 d followed by 5 d of recovery on regular water. Using this experimental paradigm, we observed increased severity of disease in male and female C57BL/6J mice housed at 22 °C, as determined by changes in body mass, colon shortening, histopathology, and the colitis pathology score (Fig. 1 *H–J* and *SI Appendix*, Fig. S4 *A–C*). The application of reaction norms confirmed presence of higher disease tolerance in thermoneutral mice (Fig. 1*K* and *SI Appendix*, Fig. S4*D*). Second, we orally infected susceptible C3H/HeJ female mice with *Citrobacter rodentium* (strain DSB100), a

Gram-negative attaching and effacing pathogen that causes transmissible colonic hyperplasia and colitis (15). While infection of C3H/HeJ mice with *C. rodentium* resulted in rapid weight loss and mortality (100%) in mice housed at 22 °C, thermoneutral housing significantly attenuated disease severity and mortality in these animals (Fig. 1 *L* and *M*). Because bacterial burden in cecum and colon was similar between the two groups (Fig. 1*N* and *SI Appendix*, Fig. S4*E*), it suggests that thermoneutral C3H/HeJ mice are more tolerant to infection with *C. rodentium*. Taken together, our data demonstrate that intestinal disease tolerance is expressed in thermoneutral mice, which decreases the severity of noninfectious and infectious colitogenic diseases.

To understand the mechanisms that regulate intestinal disease tolerance, we first focused on mucosal immunity and the microbiota, which are critical regulators of intestinal health (16, 17). Systematic profiling of lamina propria mucosal immune cells revealed higher numbers of IFNγ$^+$ and IL-17$^+$ cells and innate immune cells, including monocytes, neutrophils, MHCII$^+$CD11c$^+$ dendritic cells, and F4/80$^+$CD11b$^+$ macrophages, in mice housed at 22 °C that were treated with DSS (Dataset S1 and *SI Appendix*, Fig. S5), findings that are consistent with presence of cryptitis and mucosal inflammation in these animals (Fig. 1*D*). In support of this observation, concentrations of IL-6, MCP-1, and IFNγ, but not IL-12p70 and TNF, were higher on day 7 in colonic tissue of mice housed at 22 °C (*SI Appendix*, Fig. S6 *A–E*). In contrast, numbers of regulatory T cells (Tregs), CD4$^+$ and γδ T cells, and innate lymphoid cells (ILC1, ILC2, and ILC3), which secrete IL-10, amphiregulin, and IL-22 to maintain intestinal barrier function and microbial homeostasis (18), were not significantly higher in the colons of thermoneutral mice (Dataset S1 and *SI Appendix*,

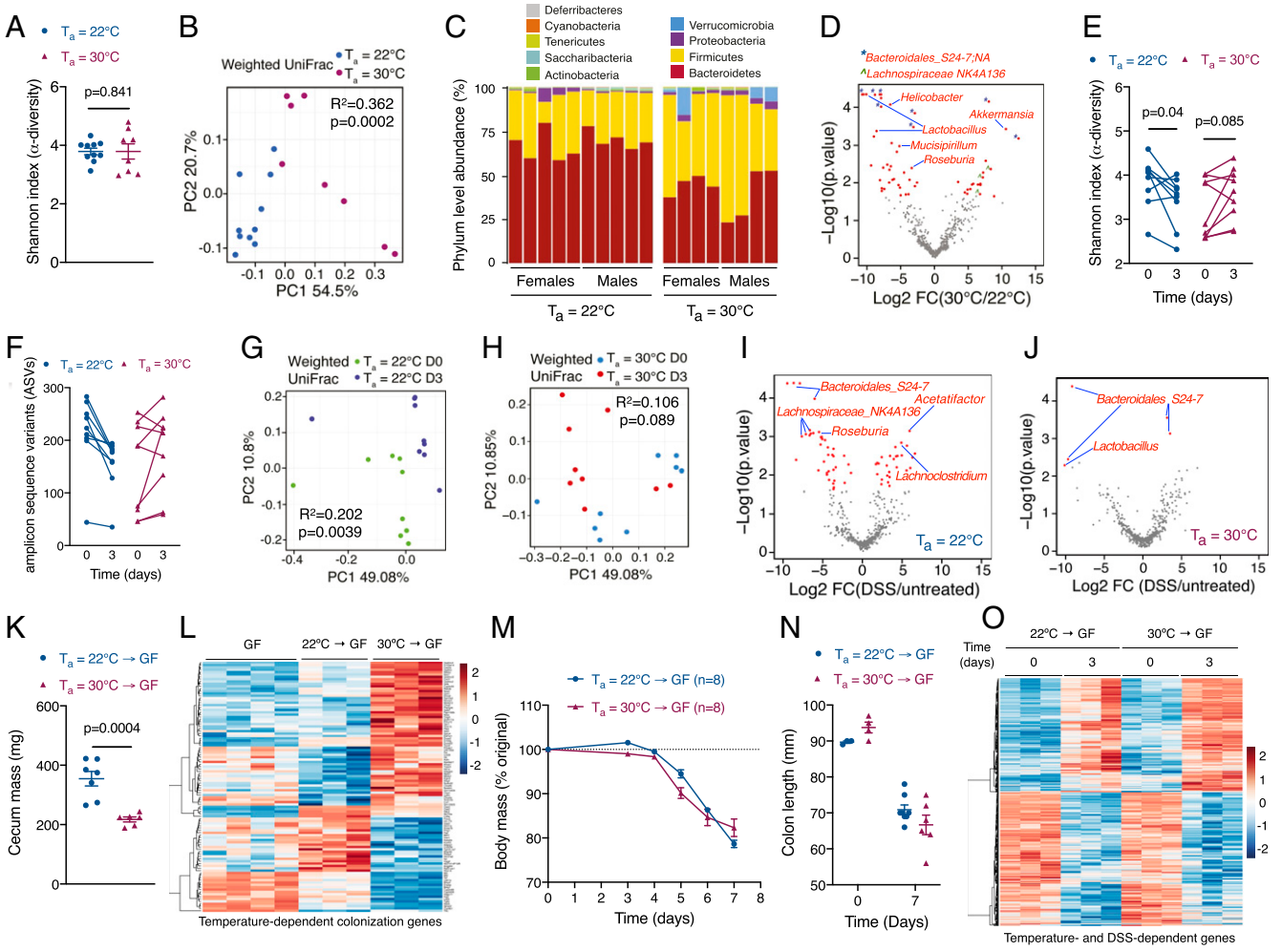

Fig. 2. Gut microbiota is not sufficient to induce intestinal disease tolerance. (*A–D*) Fecal 16S rRNA sequencing was performed from C57BL/6J male and female mice housed at T_a = 22 °C or T_a = 30 °C (n = 8 to 10 per temperature; data representative of n = 2 independent experiments). (*A*) Alpha diversity was measured by the Shannon index (analyzed by Wilcoxon signed-rank test, P = 0.841). (*B*) Beta diversity was measured by weighted UniFrac distance metric (analyzed by ADONIS, R^2 = 0.362, P = 0.0002 comparing temperature). (*C*) Phylum-level relative abundance of fecal microbiota. (*D*) Volcano plot depicting relative abundance of sequence variants [analyzed by ALDEx2 with Wilcoxon rank-sum test, log2 fold change >1 and false discovery rate (FDR) <0.1]. (*E–J*) Fecal 16S rRNA sequencing was performed in C57BL/6J male and female mice treated with DSS for 3 d (n = 9 per time point and temperature). (*E*) Alpha diversity was measured by the Shannon index (analyzed by paired t test). (*F*) Number of observed amplicon sequence variants (ASVs) at T_a = 22 °C and T_a = 30 °C. (*G* and *H*) Beta-diversity was measured by weighted UniFrac distance metric at T_a = 22 °C (*G*; analyzed by ADONIS, R^2 = 0.202, P = 0.004 comparing treatment) or T_a = 30 °C (*H*; analyzed by ADONIS, R^2 = 0.106, P = 0.089 comparing treatment). (*I* and *J*) Volcano plots of significantly altered ASVs after DSS treatment at T_a = 22 °C (*I*) or T_a = 30 °C (*J*) analyzed by ALDEx2 with Wilcoxon rank-sum test, log2 fold change >1 and FDR <0.1. (*K–O*) GF mice were reconstituted with cecal contents of C57BL/6J mice housed at T_a = 22 °C or T_a = 30 °C. Two weeks after colonization, reconstituted mice were treated with 4% DSS in drinking water for 7 d. Cecal mass (*K*), body mass (*M*), and colon length (*N*) of treated mice (representative of n = 2 independent experiments). In each group, three mice were euthanized or died between days 6 and 7. (*L* and *O*) Heat map of differentially expressed genes in GF and microbiota colonized mice at baseline (*L*) and after colitis (*O*; n = 3 to 4 per time point and temperature, fold change ≥1.5, adjusted P value <0.05). Data are presented as mean ± SEM.

Fig. S6 *F–H*). These findings are consistent with immunity's primary role in resistance rather than disease tolerance (1).

Gut Microbiota Is Not Sufficient to Induce Intestinal Disease Tolerance in Mice Housed at Subthermoneutrality. We next asked whether the gut microbiota participates in intestinal disease tolerance. The 16S rRNA gene sequencing (16S-seq) of fecal samples revealed that diversity was similar between mice housed at 22 °C and 30 °C (Fig. 2*A*). In contrast, principal coordinates analysis of weighted UniFrac distances revealed a significant difference in microbial composition between mice housed at 22 °C and 30 °C (Fig. 2*B*). Firmicutes and Verrucomicrobia phyla were increased, whereas Bacteroidetes phylum was decreased, in fecal samples of thermoneutral mice (Fig. 2*C*). Of note, several genera implicated in promotion of mucosal inflammation and colitis, such as *Helicobacter* and *Mucispirillum*, were higher in fecal samples of mice housed at 22 °C (Fig. 2*D*) (19, 20). These shifts in the gut microbiota of thermoneutral mice were accompanied by a modest increase (10 to 16%) in goblet cells (*SI Appendix*, Fig. S6 *I* and *J*), which secrete mucus to form a barrier between the intestinal epithelial cells and microbiota.

Based on these findings, we next asked how the microbiome responded to DSS-induced intestinal injury. Compared to thermoneutral mice, the fecal microbiota became destabilized in mice at subthermoneutrality after treatment with DSS, as evidenced by loss of microbial diversity, reduction in richness, and an increase in the phylogenetic distance (Fig. 2 *E–H*). For example, statistical analysis of weighted UniFrac distances revealed a significant effect of DSS treatment in mice housed at 22 °C ($P = 0.0039$, $R^2 = 0.202$), but not in mice housed at 30 °C ($P = 0.089$, $R^2 = 0.106$; ADONIS with mouse identifier as strata). The resilience of thermoneutral microbial communities to DSS-induced intestinal injury was also seen at the genus level. For example, a number of butyrate-producing genera, including *Roseburia* and *Lachnospiraceae_NK4A136*, were reduced in fecal samples of mice housed at 22 °C (Fig. 2 *I* and *J*). These data together suggest that microbial communities in the colon of thermoneutral mice are not only distinct, but also resilient to perturbations caused by injury to the intestinal epithelium.

To test whether microbiome regulates intestinal tolerance, we colonized germ-free (GF) mice housed at 22 °C with cecal contents isolated from C57BL/6J mice housed at 22 °C or 30 °C and then treated them with DSS. The 16S-seq of fecal samples from colonized GF mice revealed 15 of 16 recipients were efficiently colonized with the donor microbiota, as evidenced by phylum composition and beta diversity (*SI Appendix*, Fig. S7 *A* and *B*). However, alpha diversity (species richness) was reduced in GF mice colonized with microbiota from thermoneutral (30 °C → GF) mice (*SI Appendix*, Fig. S7*C*), suggesting that interactions between the colonic niche and microbiota are critical for maintenance of richness in gut microbial communities.

While colonization of GF mice with cecal contents of thermoneutral mice (30 °C → GF) led to significant changes in cecum size and intestinal epithelial cell (colonocyte) transcriptome, the latter was assessed by RNA sequencing (RNA-seq) on isolated colonocytes (Fig. 2 *K* and *L*), and there was no difference between the two groups in development of colitis, as determined by changes in body mass and colon length (Fig. 2 *M* and *N* and *SI Appendix*, Fig. S7*D*). Consistent with these observations, a majority of temperature- and colonization-dependent genes remained unchanged after DSS-induced injury (*SI Appendix*, Fig. S7*E* and Fig. 2*L*), whereas the expression pattern of DSS-dependent genes was similar across the two groups of colonized mice (Fig. 2*O*). These results suggest that the disease-tolerance phenotype of thermoneutral mice is not transferable by the gut microbiota to mice housed at subthermoneutrality (22 °C). However, since we were unable to perform reciprocal colonization experiments in thermoneutral GF mice, we cannot exclude the possibility that the microbiota of mice housed at subthermoneutrality might negatively impact the expression of disease tolerance in thermoneutral mice.

Intestinal Injury Reprograms Colonocytes to Promote Disease Tolerance. The tolerance capacity of tissues is regulated by their susceptibility to damage, renewal rate, and functional autonomy (1). Because the intestinal epithelium has high regenerative capacity, we next asked whether intrinsic differences in the rate of cellular renewal might contribute to higher disease tolerance in thermoneutral mice. To test this hypothesis, we quantified the number of $Lgr5^+$ cells, which are necessary for homeostatic replacement of enterocytes and secretory cells in the villi (21). Although the number of $Lgr5^+$ cells was slightly higher in uninjured colons of thermoneutral mice (*SI Appendix*, Fig. S8 *A* and *B*), their contribution to epithelial renewal after injury was similar between mice housed at 22 °C or 30 °C (Fig. 3 *A* and *B*). Moreover, the numbers of $GLI1^+$ mesenchymal cells, which provide WNT2B to support proliferation of intestinal stem cells (22); $SCA1^+$ cells, which activate a fetal development program to mediate intestinal repair (23); and $Ki67^+$ proliferating cells were not higher in the crypts and villi of thermoneutral mice (*SI Appendix*, Fig. S8 *C–H*). In agreement with these data, RNA-seq of isolated intestinal crypts revealed that the transcriptional response to injury was modest and largely similar between the two groups of mice (Fig. 3*C* and *SI Appendix*, Fig. S9 *A–D*). Taken together, these findings suggest that differences in the rate of cellular renewal are unlikely to account for the higher disease tolerance of thermoneutral mice.

We then asked whether intestinal disease tolerance might be mediated by basal or inducible responses in colonocytes. RNA-seq of purified colonocytes revealed that, while the basal states were similar between the two groups of mice, their response to injury was dramatically different (Fig. 3*D* and *SI Appendix*, Fig. S9 *A–D*). Unlike the changes in the intestinal crypts (Fig. 3*C*), injury led to marked remodeling of colonocyte transcriptome in thermoneutral mice, as evidenced by repression of 3,002 genes and induction of 1,998 genes. Gene Ontology (GO) enrichment analysis revealed that processes associated with histone modification, DNA damage, and cell cycle were down-regulated, whereas those associated with mitochondria, peptide and nucleotide metabolism, oxidative phosphorylation, and the tricarboxylic acid (TCA) cycle were induced in colonocytes of thermoneutral mice (Fig. 3*D* and *SI Appendix*, Fig. S9 *E* and *F*). Together, these data suggest that injury reprograms the colonocytes for oxidative metabolism in thermoneutral mice.

Recent studies have demonstrated that microbiota-derived butyrate activates peroxisome proliferator-activated receptor γ to promote oxidative metabolism in colonocytes, which maintains a hypoxic epithelial niche to prevent microbial dysbiosis and epithelial damage (17, 24). To investigate whether this occurs in the colonocytes of thermoneutral mice, we quantified metabolites in cecal contents of mice housed at 22 °C or 30 °C. We found that butyrate was significantly increased in the cecal contents of thermoneutral mice after DSS-induced injury (Fig. 3*E*), findings that are consistent with the reduction in butyrate-producing genera in mice housed at subthermoneutrality (Fig. 2*I*). Staining with pimonidazole revealed that colonocyte surface hypoxia was reduced in mice housed at 22 °C, whereas it was preserved in thermoneutral mice after injury (Fig. 3 *F* and *G*). This shift of colonocytes to oxidative metabolism resulted in higher disease tolerance during injury, as determined by reduction in number of $TUNEL^+$ apoptotic cells in the villi (Fig. 3*H* and *SI Appendix*, Fig. S8*I*).

Because transcriptional signatures for DNA damage, mitosis, and cell division were decreased in colonocytes of thermoneutral mice after injury (Fig. 3*D* and *SI Appendix*, Fig. S9*F*), we next asked whether thermoneutral mice were more tolerant to inflammation-induced colon tumorigenesis. Using a mouse model of colorectal cancer in which DSS-induced inflammation promotes tumorigenesis (25), we found that male and female

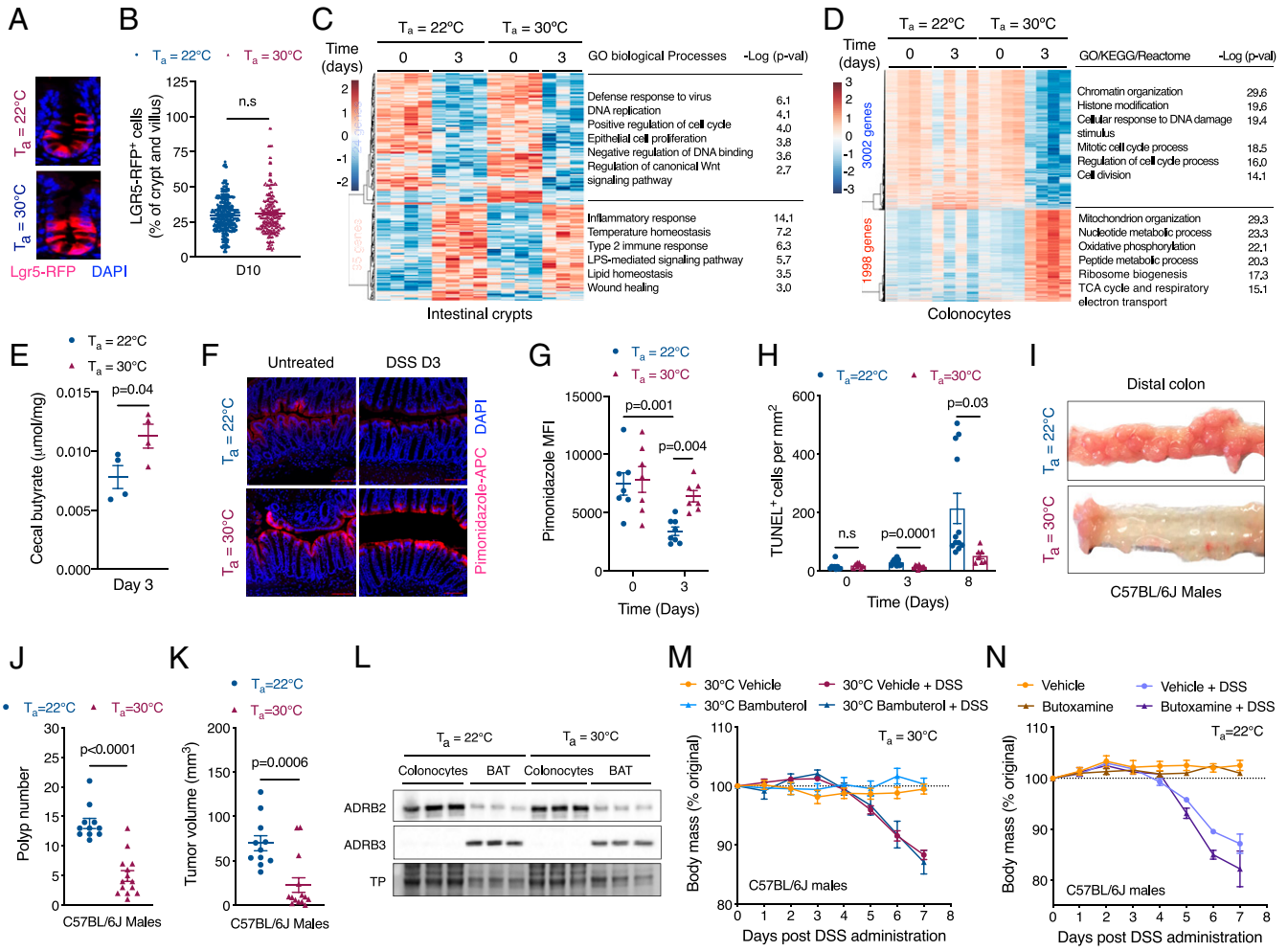

Fig. 3. Injury-induced reprogramming of colonocytes promotes disease tolerance. (*A* and *B*) Immunofluorescence for Lgr5-RFP$^+$ cells during the regenerative phase of DSS-induced tissue injury. *Lgr5*$^{GFP\text{-}ires\text{-}creERT2/+}$*Rosa26*$^{RFP/+}$ mice housed at T_a = 22 °C or T_a = 30 °C were treated with DSS for 5 d and then switched to regular water. Mice were injected with tamoxifen on D7, and Lgr5-RFP$^+$ cells were quantified on D10. Representative images (*A*) and quantification of LGR5-RFP$^+$ cells per crypt and villus unit (*B*; n = 261 to 348 crypt and villus units quantified per condition; data pooled from n = 2 independent experiments and analyzed using Student's t test). (*C* and *D*) Heat map, GO enrichment analysis, and corresponding P values of differentially expressed genes in intestinal crypts (*C*) and colonocytes (*D*) of C57BL/6J male mice administered DSS at T_a = 22 °C and T_a = 30 °C (n = 3 to 4 per time point and temperature, fold change ≥1.5, adjusted P value <0.05). (*E*) Quantification of cecal butyrate in C57BL/6J male mice administered DSS at T_a = 22 °C and T_a = 30 °C (n = 4 per time point and temperature). (*F* and *G*) Staining for colonocyte hypoxia using pimonidazole in C57BL/6J male mice administered DSS at T_a = 22 °C and T_a = 30 °C. Representative images (*F*) and quantification of hypoxia staining (*G*) in colonocytes (n = 7 to 8 per time point and temperature, data pooled from n = 2 independent experiments and analyzed by Student's t test). (*H*) Quantification of TUNEL$^+$ apoptotic cells in colon of C57BL/6J male mice administered DSS at T_a = 22 °C and T_a = 30 °C (n = 7 to 12 per time point and temperature; data pooled from n = 3 independent experiments and analyzed by Student's t test). (*I*–*K*) To induce colon cancer, C57BL/6J male mice housed at T_a = 22 °C and T_a = 30 °C were administered a single dose of azoxymethane (AOM) followed by three cycles of DSS. Gross histology (*I*), polyp number (*J*), and tumor volume (*K*) in treated mice (n = 11 to 14 per temperature; data pooled from n = 2 independent experiments and analyzed by Student's t test). (*L*) Immunoblotting for β2- and β3-adrenergic receptors in colonocytes and BAT of C57BL/6J male mice administered DSS at T_a = 22 °C and T_a = 30 °C. TP, total protein. (*M*) Body mass of male C57BL/6J mice at T_a = 30 °C during DSS-induced colitis that were pretreated with β2-adrenoreceptor agonist bambuterol (n = 5 to 8 per condition; data analyzed by two-way ANOVA). (*N*) Body mass of male C57BL/6J mice at T_a = 22 °C during DSS-induced colitis that were pretreated with β2-adrenoreceptor antagonist butoxamine (n = 4 to 5 per condition; data analyzed by two-way ANOVA). Data are presented as mean ± SEM.

thermoneutral mice were more tolerant to the development of colon polyps, as determined by quantification of polyp number and tumor volume (Fig. 3 *I*–*K* and *SI Appendix*, Fig. S9 *G* and *H*). In aggregate, these data suggest that the disease-tolerant phenotype of thermoneutral mice is likely mediated by transcriptional reprogramming of colonocytes during injury, which maintains a hypoxic niche to prevent microbial dysbiosis and tissue damage.

To identify mechanisms that regulate transcriptional reprogramming of colonocytes during injury, we focused on adrenergic signaling pathways because thermoneutral housing decreases adrenergic tone in mice (13). Since colonocytes express β2-adrenergic receptor (Fig. 3*L* and *SI Appendix*, Fig. S10*A*), which has been implicated in intestinal homeostasis (26), we treated mice housed at 22 °C or 30 °C with the long-acting β2-adrenergic agonist bambuterol. To our surprise, treatment of mice with bambuterol did not affect disease tolerance during DSS-induced colitis (Fig. 3*M* and *SI Appendix*, Fig. S10 *B*–*N*). Similar results were obtained when mice housed at 22 °C or 30 °C were treated with the β2 receptor-selective antagonist butoxamine (Fig. 3*N* and *SI Appendix*, Fig. S11 *A*–*F*), indicating that β2-adrenergic signaling does not contribute to decreased disease tolerance in mice housed under subthermoneutral conditions.

Adrenergic Activation of Thermogenic Fat Regulates Colonocyte Gene Expression and Intestinal Disease Tolerance. Mice housed under a subthermoneutral environment activate adaptive thermogenesis via the β3-adrenergic receptor in brown and beige adipocytes to maintain homeothermy (27). We thus asked whether treatment of thermoneutral mice with CL 316,243, a β3 receptor-selective agonist, affects intestinal disease tolerance. Administration of CL 316,243 to thermoneutral mice activated thermogenesis in brown adipose tissue (BAT), which increased energy expenditure without affecting locomotor activity (Fig. 4 *A–C* and *SI Appendix*, Fig. S12*A*). Consistent with these observations, we observed that BAT mass was reduced in thermoneutral mice treated with the β3 agonist CL 316,243 but not the β2 agonist bambuterol (*SI Appendix*, Fig. S10 *C* and *J* and S12 *B* and *G*). This increase in peripheral energy expenditure was sufficient to decrease disease tolerance in thermoneutral male and female mice, as determined by a reduction in body mass and colon shortening during DSS-induced colitis (Fig. 4 *D* and *E*, and *SI Appendix*, Fig. S12 *C–F*). These inhibitory effects of CL 316,243 on intestinal disease tolerance were also observed in the regenerative paradigm of experimental colitis (*SI Appendix*, Fig. S12 *H* and *I*), whereas inhibition of ADRB3 signaling with the β3-adrenergic antagonist SR59203A improved disease tolerance to DSS-induced colitis in mice housed at subthermoneutrality (*SI Appendix*, Fig. S12 *J–L*).

We next asked whether treatment with CL 316,243 affected basal and injury-induced immune responses in the colon. Analysis of inflammatory cytokines revealed modest changes in in colon and serum of mice during the time course of DSS-induced colitis (*SI Appendix*, Fig. S13 *A–L*). In contrast, flow cytometric analysis of lamina propria cells revealed increased numbers of innate (neutrophils, monocytes, eosinophils, and natural killer cells), adaptive ($CD4^+$ cells, $CD8^+$ cells, and $FoxP3^+$ Tregs), and innate lymphoid cells in mice administered CL 316,243 (*SI Appendix*, Fig. S14 *A–I*). Because these changes in immune cell numbers were also observed in the lamina propria of CL 316,243-treated mice receiving vehicle (*SI Appendix*, Fig. S14 *A–I*), it suggests that activation of thermogenesis alters the basal state of the colonic epithelia.

To gain insights into how treatment with CL 316,243 alters intestinal homeostasis, we performed RNA-seq on colonocytes. Principal component analysis (PCA) revealed that colonocytes of CL 316,243-treated thermoneutral mice clustered separately from those treated with vehicle (Fig. 4*F*). For example, compared to vehicle-treated thermoneutral controls (D0), the transcriptome of D0 colonocytes from CL 316,243-treated mice was similar to that of mice housed at subthermoneutrality and administered DSS for 3 d (Fig. 4 *F* and *G*). Furthermore, GO enrichment analysis revealed that biological processes associated with inflammation, cytokine production, and apoptosis were increased, whereas those associated with morphogenesis, DNA damage, TGF-β and Hippo signaling, and stem cell maintenance (including *Hopx*, *Lgr5*, *Axin2*, *Ascl2*) were decreased in colonocytes of thermoneutral mice administered CL 316,243 (Fig. 4*G*). These findings suggest that activation of thermogenic adipocytes by CL 316,243 results in transcriptional reprogramming of colonocytes.

We next asked whether CL 316,243-induced transcriptional changes in colonocytes were sufficient to alter the composition of the gut microbiota. The 16S-seq revealed that treatment with CL 316,243 increased the diversity and changed the composition of gut microbial communities (Fig. 4 *H* and *I*). Although the composition of the gut microbiota of mice administered CL 316,243 was distinct from mice housed at 22 °C or 30 °C (Fig. 4*H*), it was enriched in two colitogenic genera, *Helicobacter* and *Mucispirillum*, that were also abundant in mice housed at subthermoneutrality (Figs. 4*J* and 2*D*). This CL 316,243-induced shift in colonocyte gene expression and microbial diversity was sufficient to decrease colonocyte surface hypoxia after DSS-induced injury (Fig. 4 *K* and *L*).

To address the possibility that β3-adrenergic signaling might directly regulate colonocyte renewal, we cultured colonoids from mice housed at 22 °C or 30 °C and treated them with β3 agonist CL 316,243. Consistent with higher numbers of $Lgr5^+$ cells in uninjured colons of thermoneutral mice (*SI Appendix*, Fig. S8 *A* and *B*), crypts isolated from thermoneutral mice yielded larger number of colonoids, which were also larger in size (*SI Appendix*, Fig. S15 *A–C*). Crypt budding, a marker of intestinal stem cell renewal, was also higher in cultures derived from mice housed at 30 °C (*SI Appendix*, Fig. S15*D*). In agreement with predominant expression of β2-adrenergic receptor in colonic crypts (*SI Appendix*, Fig. S15*E*), treatment with the β3 agonist CL 316,243 did not significantly affect size or budding of cultured colonoids (*SI Appendix*, Fig. S15 *C* and *D*). However, we observed that CL 316,243 treatment led to a modest reduction in the number of cultured colonoids from thermoneutral mice, which was not associated with a decrease in their viability (*SI Appendix*, Fig. S15 *B*, *F*, and *G*). Together, these data suggest that activation of β3-adrenergic signaling by CL 316,243 likely modulates disease tolerance to DSS-induced colitis in an indirect manner.

Adrenergic Signaling in Thermogenic Adipocytes Regulates Intestinal Disease Tolerance. To investigate whether DSS-induced colitis alters the transcriptional response of thermogenic adipocytes, we performed RNA-seq on BAT, which is enriched in β3-adenergic receptor-positive thermogenic adipocytes (Fig. 3*L*). We found that BAT transcriptome underwent dramatic changes at both the early (day [D] 3) and late (D7) stages of colitis, which were dependent on the adrenergic state of the animals (Fig. 5*A* and *SI Appendix*, Fig. S15*H*). GO enrichment analysis revealed that processes associated with inflammatory response, cytokine production, myeloid leukocyte activation, and response to wounding were enriched among the induced genes, whereas those associated with oxidative phosphorylation, respiratory electron transport, and ATP metabolic process were enriched among the repressed genes in BAT of thermoneutral mice after DSS-induced injury (Fig. 5*A*). In agreement with these RNA-seq data, treatment with DSS suppressed the rate of oxygen consumption in BAT of thermoneutral, but not subthermoneutral, mice (*SI Appendix*, Fig. S15*I*). In aggregate, these data demonstrate that BAT dynamically responds to DSS-induced colonic injury, implicating it in the modulation of intestinal disease tolerance in mice housed in a subthermoneutral environment.

To determine whether β-adrenergic signaling in thermogenic adipocytes regulates intestinal disease tolerance, we used $Gnas^{f/f}Adipoq^{Cre}$ mice, which lack guanine nucleotide-binding alpha-stimulating protein (*Gnas*) that is required for β-adrenergic activation of thermogenic adipocytes during cold stress (28). We chose $Gnas^{f/f}Adipoq^{Cre}$ rather than $Gnas^{f/f}Ucp1^{Cre}$ mice for these studies because UCP1 is expressed by tissue-resident alternatively activated macrophages (29), which participate in tissue repair (30). Because $Gnas^{f/f}$ mice were on mixed genetic background (129S6/SvEvTac*-Black Swiss), we first asked whether strain background affected expression of intestinal disease tolerance at thermoneutrality. We observed that $Gnas^{f/f}$ mice at thermoneutrality were more tolerant to DSS-induced colitis (*SI Appendix*, Fig. S16 *A* and *B*), indicating that thermoneutral housing is sufficient to elicit the disease tolerance phenotype across multiple mouse strains.

Based on these findings, we asked whether loss of adrenergic signaling in thermogenic adipocytes affected intestinal disease tolerance. We found that $Gnas^{f/f}Adipoq^{Cre}$ mice were more tolerant to DSS-induced colitis under subthermoneutral conditions (22 °C), as evidenced by reduced weight loss, colon shortening, and colitis pathology scores in $Gnas^{f/f}Adipoq^{Cre}$ mice (Fig. 5 *B* and *C* and *SI Appendix*, Fig. S16*C*). This improvement in disease fitness was associated with increased mass of brown and white adipose tissues in $Gnas^{f/f}Adipoq^{Cre}$ mice (Fig. 5*D* and *SI Appendix*, Fig. S16 *D* and *E*), findings that are consistent with loss of adrenergic signaling in these fat depots (28).

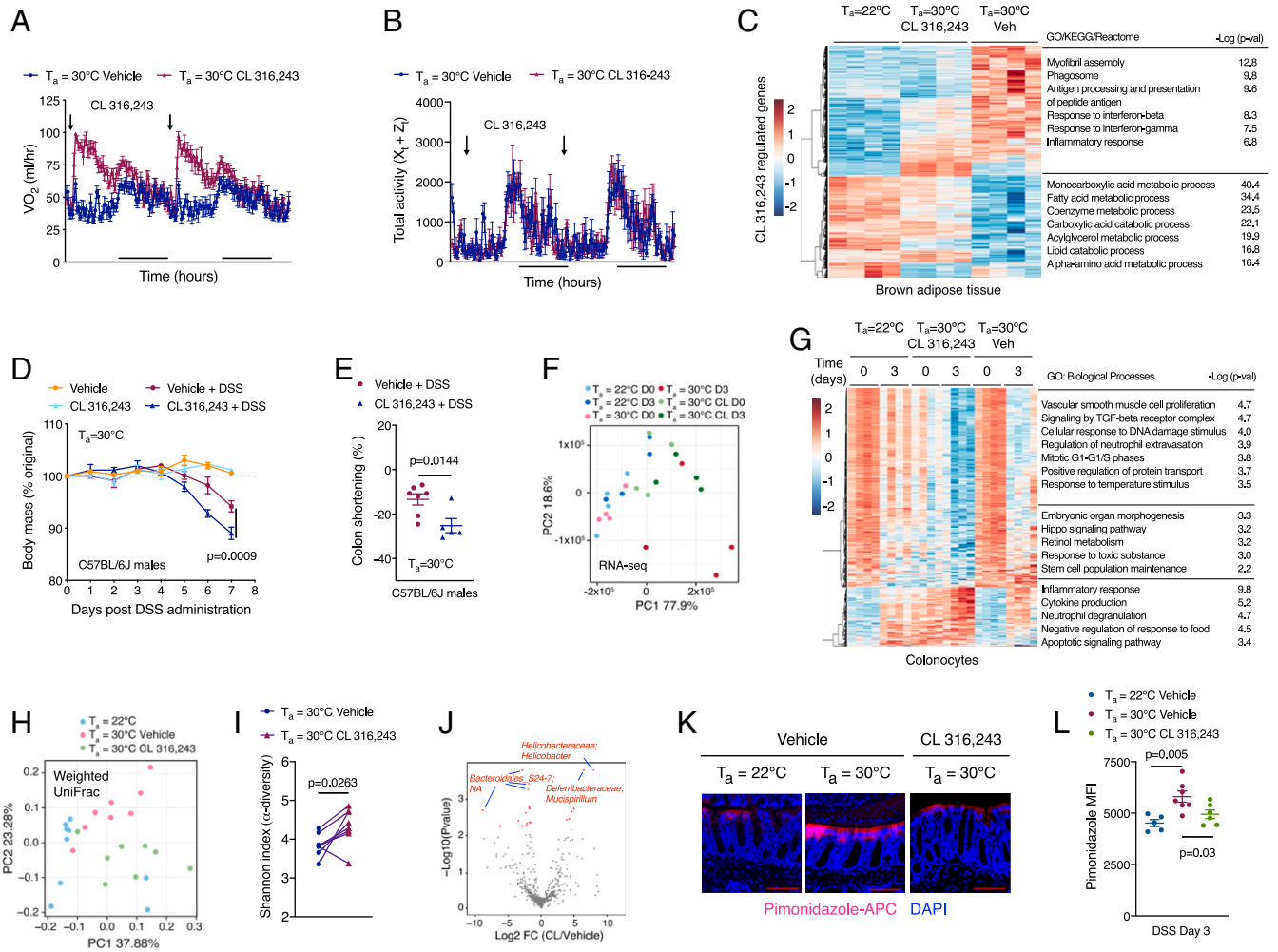

Fig. 4. Adrenergic activation of thermogenic fat regulates colonocyte gene expression and intestinal disease tolerance. (*A* and *B*) Thermoneutral C57BL/6J female mice were treated with β3-adrenoreceptor agonist CL 316,243 or vehicle for 3 wk. Rate of oxygen consumption (VO_2; *A*) and total activity (*B*) in female mice housed at T_a = 30 °C and treated with vehicle or CL 316,243 (n = 4 to 5 per treatment). (*C*) Heat map, GO enrichment analysis, and corresponding *P* values of differentially expressed genes in BAT of CL 316,243 and DSS-treated C57BL/6J male mice housed at T_a = 22 °C or T_a = 30 °C (n = 4 per temperature and condition, fold change ≥1.5, adjusted *P* value <0.05). (*D* and *E*) C57BL/6J male mice were treated with β3-adrenoreceptor agonist CL 316,243 for 2 wk at T_a = 30 °C prior to administration of DSS. Body mass (*D*) and colon shortening (*E*) in treated mice [n = 4 to 8 per condition; data analyzed by two-way ANOVA (*D*) and Student's *t* test (*E*)]. (*F*) PCA of colonocyte transcriptomes from male C57BL6/J mice housed at T_a = 22 °C or T_a = 30 °C and treated with CL 316,243. Each dot indicates an individual biological replicate (n = 4 per temperature and condition). (*G*) Heat map, GO enrichment analysis, and corresponding *P* values of differentially expressed genes in colonocytes of C57BL/6J male mice treated with vehicle or CL 316,243 and administered DSS at T_a = 22 °C and T_a = 30 °C (n = 4 per temperature and condition, fold change ≥1.5, adjusted *P* value <0.05). (*H–J*) 16S rRNA-sequencing was performed on fecal samples from C57BL/6J male and female mice that were treated with CL 316,243 or vehicle for 3 wk (n = 9 per time point and temperature). Beta diversity was measured by weighted UniFrac (*H*; analyzed by ADONIS, T_a = 22 °C vs. T_a = 30 °C vehicle, R^2 = 0.2227, P = 0.0016; 30 °C vehicle vs. 30 °C CL 316,243, R^2 = 0.1952, P = 0.0096; 22 °C vs. 30 °C CL 316,243, R^2 = 0.1914, P = 0.0133), alpha diversity was measured by the Shannon index (*I*; analyzed by paired Student's *t*-test), and a volcano plot depicts significantly altered sequencing variants after treatment with CL 316,243 at T_a = 30 °C (*J*; analyzed by ALDEx2 with Wilcoxon rank-sum test, log2 fold change >1 and FDR <0.1). (*K* and *L*) Representative images (*K*) and quantitation (*L*) of pimonidazole staining of the large intestine in C57BL6/J male mice treated with β3-adrenoreceptor agonist CL 316,243 or vehicle at T_a = 22 °C or T_a = 30 °C and DSS for 3 d (n = 5 to 7 per group, analyzed by Student's *t* test). Data are presented as mean ± SEM.

We next asked whether the inhibitory effects of CL 316,243 on intestinal disease tolerance required β-adrenergic signaling in thermogenic adipocytes. Compared to littermate controls, *Gnas*$^{f/f}$*Adipoq*^{Cre} mice were protected from the negative effects of CL 316,243 on intestinal disease tolerance, as determined by body mass, histopathology, and mass of brown and white adipose tissues (Fig. 5 *E* and *F* and *SI Appendix*, Fig. S16 *F–L*). These findings suggested that adrenergic activation of thermogenic adipocytes might release factors (nucleic acid-based, proteinaceous, or small molecules) that regulate intestinal disease tolerance. One potential factor linking adrenergic activation of BAT to intestinal disease tolerance is IL-6, which is released by BAT in response to environmental stressors (31). However, we found that neutralization of IL-6 did not improve disease tolerance to experimental colitis in mice housed at subthermoneutrality (*SI Appendix*, Fig. S17 *A–F*).

To take an unbiased approach for identification of potential mediators of intestinal disease tolerance, we analyzed the expression of secreted factors in BAT. We found that DSS-induced colitis increased expression of *Mfge8*, *Grn*, and *Apln* in BAT of thermoneutral mice (Fig. 5*G*, *SI Appendix*, Fig. S15*J*, and Dataset S2), which have previously been implicated in suppressing colonic inflammation and tissue damage (32–34). Furthermore, RNA-seq

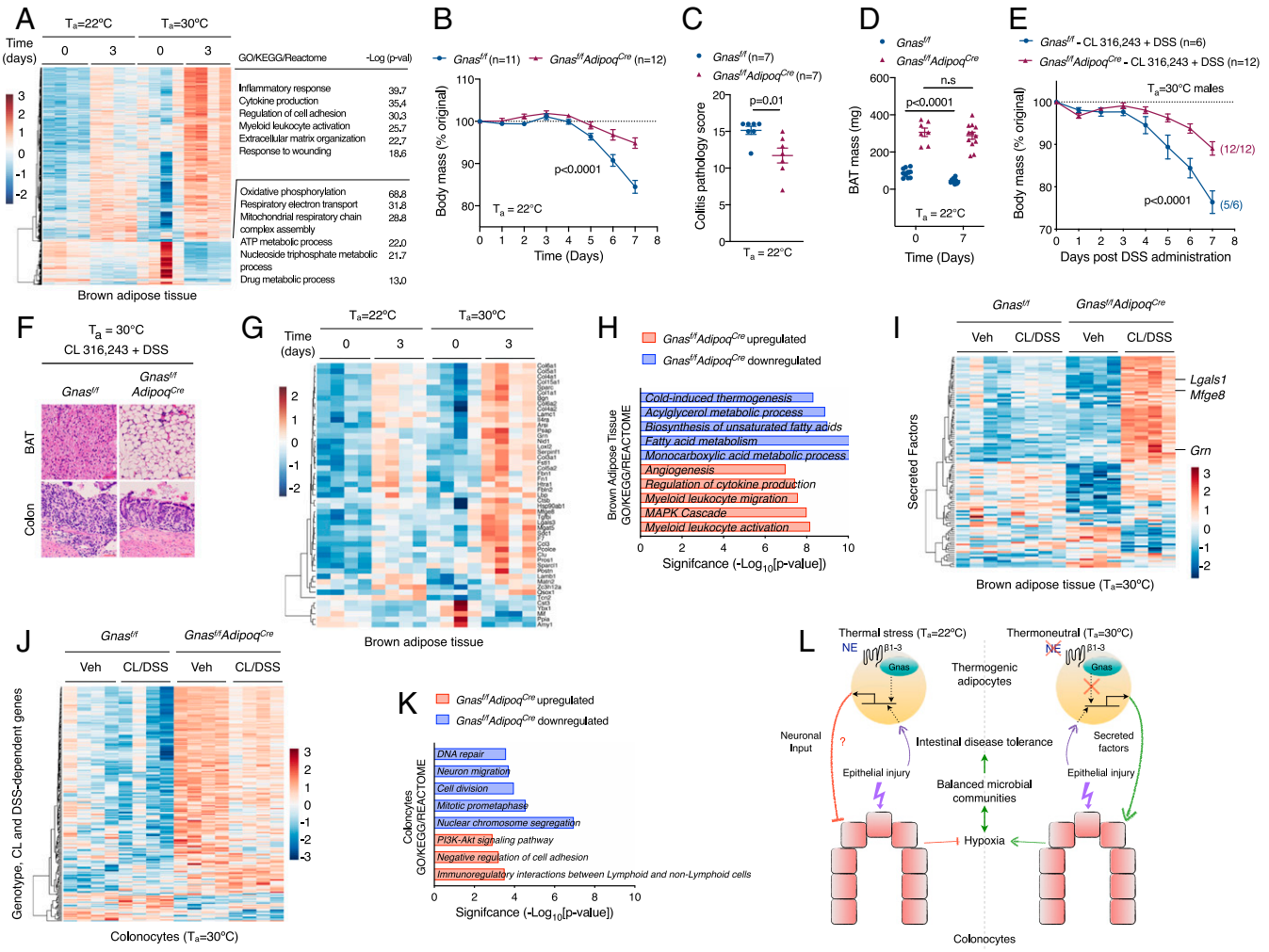

Fig. 5. Adrenergic signaling in thermogenic adipocytes regulates intestinal disease tolerance. (*A*) Heat map, GO enrichment analysis, and corresponding *P* values of differentially expressed genes in BAT of C57BL/6J male mice that were administered DSS at T_a = 22 °C and T_a = 30 °C (n = 4 per time point and condition, fold change ≥1.5, adjusted *P* value <0.05). (*B–D*) Colitis was induced with 3% DSS in male and female *Gnas*$^{f/f}$ and *Gnas*$^{f/f}$*Adipoq*^{Cre} mice housed at T_a = 22 °C. Body mass (*B*; n = 11 to 12 per genotype; data pooled from n = 2 independent experiments and analyzed by two-way ANOVA), colitis pathology score (*C*; n = 7 per genotype and analyzed by Student's t test), and BAT mass (*D*; n = 7 to 12 per genotype; data pooled from n = 2 independent experiments and analyzed by Student's t test). (*E* and *F*) Colitis was induced with 4% DSS in male and female *Gnas*$^{f/f}$ and *Gnas*$^{f/f}$*Adipoq*^{Cre} mice housed at T_a = 30 °C that were treated with CL 316,243. Body mass (*E*; n = 6 to 12 per genotype; data pooled from n = 2 independent experiments and analyzed by two-way ANOVA) and representative pictures of H&E-stained sections of BAT and colon (*F*). (Scale bar: 100 μM.) (*G*) Heat map of differentially expressed secreted factors in BAT of C57BL/6J male mice housed at T_a = 22 °C and T_a = 30 °C that were administered DSS for 3 d (n = 4 per time point and condition, fold change ≥1.5, adjusted *P* value <0.05). (*H–K*) RNA-seq analysis of BAT and colonocytes isolated from thermoneutral *Gnas*$^{f/f}$ and *Gnas*$^{f/f}$*Adipoq*^{Cre} mice treated with vehicle or CL 316,243 that were administered DSS for 4 d (n = 4 per condition, fold change ≥1.5, adjusted *P* value <0.05). GO enrichment analysis (*H*) of up-regulated and down-regulated genes in BAT of *Gnas*$^{f/f}$*Adipoq*^{Cre} mice (*H*) and heat map of secreted factors (*I*) in BAT of *Gnas*$^{f/f}$ and *Gnas*$^{f/f}$*Adipoq*^{Cre} mice. Heat map (*J*) and GO enrichment analysis (*K*) of colonocytes in thermoneutral *Gnas*$^{f/f}$ and *Gnas*$^{f/f}$*Adipoq*^{Cre} mice (n = 4 per condition, fold change ≥1.5, adjusted *P* value <0.05). (*L*) Model depicting the thermogenic fat–epithelial cell axis that regulates intestinal disease tolerance. Thermogenic adipocytes integrate adrenergic and injury signals to modulate expression of factors that promote intestinal disease tolerance in thermoneutral mice. During injury, these factors act directly or indirectly on colonocytes to maintain epithelial hypoxia, which helps to maintain balanced microbial communities in disease-tolerant thermoneutral animals. NE, norepinephrine; β1–3, β1–3 adrenergic receptors. Data are presented as mean ± SEM.

of BAT from *Gnas*$^{f/f}$ and *Gnas*$^{f/f}$*Adipoq*^{Cre} mice revealed that β3-adrenergic signaling in thermogenic adipocytes regulated expression of secreted factors, including *Mfge8*, *Grn*, and *Lgals1* (Fig. 5 *H* and *I*), which have been implicated in amelioration of colitis (33–35). The loss of *Gnas* in thermogenic adipocytes also impacted colonocyte gene expression during colitis, as evidenced by down-regulation of processes associated with DNA repair, cell division, and mitosis (Fig. 5 *J* and *K*), which were induced in colonocytes of mice housed in a subthermoneutral environment (Fig. 3*D*). In aggregate, our findings suggest the existence of a signaling axis between thermogenic adipocytes and intestinal epithelial cells that regulates disease tolerance during experimental colitis.

Discussion

One of the most surprising findings from our studies is that intestinal disease tolerance is an inducible program in colonocytes, whose expression is dynamically regulated by adrenergic signaling in thermogenic adipocytes (Fig. 5*L*). While the tolerogenic response of colonocytes was not transferrable by the gut microbiota, interactions between the epithelial cells and microbiota are likely important in maintenance of intestinal disease tolerance, as

suggested by the stability of epithelial hypoxia and microbial communities in tolerant mice. It is not clear whether a neuronal or hormonal signal is the tolerogenic factor, but it is clear that adrenergic signaling in thermogenic adipocytes is a critical determinant of intestinal disease tolerance (Fig. 5*L*).

An important implication of our work is that disease-tolerance programs actively compete for energy with other maintenance programs, resulting in their prioritization that is dependent on the inciting stimulus, environmental conditions, and physiologic state of the organism. For example, we previously reported that mice housed under a subthermoneutral environment (22 °C) abandon homeothermy to meet the energetic demands of disease tolerance during Gram-negative sepsis (12). In contrast, we find here that intestinal disease tolerance does not require a trade-off with homeothermy, but is restricted to thermoneutral mice, whose energetic demands for thermogenesis are minimal. The elucidation of cross-talk between thermogenic adipocytes and colonocytes also has important clinical implications. For instance, since adrenergic activation of thermogenic adipocytes is currently being pursued as a therapeutic strategy for the treatment of obesity (36), our findings suggest that these potential therapies might decrease intestinal disease tolerance and predispose susceptible individuals to the development of colitogenic diseases.

Materials and Methods

Experimental details on animals, isolation of colonocytes and intestinal crypts, flow-cytometric analysis of lamina propria lymphocytes, colonization and colitis studies in GF mice, immunoblotting, quantification of colonocyte hypoxia, tissue histology and immunofluorescence, energy expenditure measurements, next-generation sequencing and RNA-seq analysis, 16s rRNA gene sequencing and analysis, metabolomics, and statistical analyses for this study are described in detail in *SI Appendix, Materials and Methods*.

Data Availability. Data generated or analyzed during this study are included in this published article and its *SI Appendix* files. The RNA-seq data have been deposited in the Gene Expression Omnibus database under ID code GSE158488. The 16S rRNA-seq data have been deposited at the Sequence Read Archive (SRA) repository under BioProject PRJNA667805.

ACKNOWLEDGMENTS. We thank members of the Chawla laboratory and A. Loh for comments on the manuscript. The authors' work was supported by an Innovator Award from the Kenneth Rainin Foundation and grants from NIH (DK094641, DK101064) to A.C.; J.R.B. was supported by grants from NIH (R03 DK121061-01 and P30 DK098722) and K.M. was supported by National Health and Medical Research Council (NHMRC) (GNT1142229). The authors acknowledge support from the Pathology & Imaging Core of the University of California, San Francisco (UCSF) Liver Center (P30 DK026743) and the UCSF Gnotobiotics Core.

1. R. Medzhitov, D. S. Schneider, M. P. Soares, Disease tolerance as a defense strategy. *Science* **335**, 936–941 (2012).
2. M. P. Soares, L. Teixeira, L. F. Moita, Disease tolerance and immunity in host protection against infection. *Nat. Rev. Immunol.* **17**, 83–96 (2017).
3. R. M. Caldwell, J. F. Schafer, L. E. Compton, F. L. Patterson, Tolerance to cereal leaf rusts. *Science* **128**, 714–715 (1958).
4. E. L. Simms, J. Triplett, Costs and benefits of plant-responses to disease–Resistance and tolerance. *Evolution* **48**, 1973–1985 (1994).
5. L. Råberg, D. Sim, A. F. Read, Disentangling genetic variation for resistance and tolerance to infectious diseases in animals. *Science* **318**, 812–814 (2007).
6. S. R. Wu, P. Reddy, Tissue tolerance: A distinct concept to control acute GVHD severity. *Blood* **129**, 1747–1752 (2017).
7. A. Wang *et al.*, Opposing effects of fasting metabolism on tissue tolerance in bacterial and viral inflammation. *Cell* **166**, 1512–1525.e12 (2016).
8. S. Weis *et al.*, Metabolic adaptation establishes disease tolerance to sepsis. *Cell* **169**, 1263–1275.e14 (2017).
9. S. Rao *et al.*, Pathogen-mediated inhibition of anorexia promotes host survival and transmission. *Cell* **168**, 503–516.e12 (2017).
10. K. Cumnock *et al.*, Host energy source is important for disease tolerance to malaria. *Curr. Biol.* **28**, 1635–1642.e3 (2018).
11. H. H. Luan *et al.*, GDF15 is an inflammation-induced central mediator of tissue tolerance. *Cell* **178**, 1231–1244.e11 (2019).
12. K. Ganeshan *et al.*, Energetic trade-offs and hypometabolic states promote disease tolerance. *Cell* **177**, 399–413.e12 (2019).
13. K. Ganeshan, A. Chawla, Warming the mouse to model human diseases. *Nat. Rev. Endocrinol.* **13**, 458–465 (2017).
14. B. Chassaing *et al.*, Fecal lipocalin 2, a sensitive and broadly dynamic non-invasive biomarker for intestinal inflammation. *PLoS One* **7**, e44328 (2012).
15. D. Borenshtein, M. E. McBee, D. B. Schauer, Utility of the Citrobacter rodentium infection model in laboratory mice. *Curr. Opin. Gastroenterol.* **24**, 32–37 (2008).
16. C. A. Thaiss, N. Zmora, M. Levy, E. Elinav, The microbiome and innate immunity. *Nature* **535**, 65–74 (2016).
17. Y. Litvak, M. X. Byndloss, A. J. Bäumler, Colonocyte metabolism shapes the gut microbiota. *Science* **362**, eaat9076 (2018).
18. R. Okumura, K. Takeda, Maintenance of intestinal homeostasis by mucosal barriers. *Inflamm. Regen.* **38**, 5 (2018).
19. D. Berry *et al.*, Intestinal microbiota signatures associated with inflammation history in mice experiencing recurring colitis. *Front. Microbiol.* **6**, 1408 (2015).
20. M. C. Kullberg *et al.*, Helicobacter hepaticus triggers colitis in specific-pathogen-free interleukin-10 (IL-10)-deficient mice through an IL-12- and gamma interferon-dependent mechanism. *Infect. Immun.* **66**, 5157–5166 (1998).
21. H. Gehart, H. Clevers, Tales from the crypt: New insights into intestinal stem cells. *Nat. Rev. Gastroenterol. Hepatol.* **16**, 19–34 (2019).
22. T. Valenta *et al.*, Wnt ligands secreted by subepithelial mesenchymal cells are essential for the survival of intestinal stem cells and gut homeostasis. *Cell Rep.* **15**, 911–918 (2016).
23. Y. M. Nusse *et al.*, Parasitic helminths induce fetal-like reversion in the intestinal stem cell niche. *Nature* **559**, 109–113 (2018).
24. M. X. Byndloss *et al.*, Microbiota-activated PPAR-γ signaling inhibits dysbiotic Enterobacteriaceae expansion. *Science* **357**, 570–575 (2017).
25. T. Tanaka *et al.*, A novel inflammation-related mouse colon carcinogenesis model induced by azoxymethane and dextran sodium sulfate. *Cancer Sci.* **94**, 965–973 (2003).
26. S. Moriyama *et al.*, β_2-adrenergic receptor-mediated negative regulation of group 2 innate lymphoid cell responses. *Science* **359**, 1056–1061 (2018).
27. M. Harms, P. Seale, Brown and beige fat: Development, function and therapeutic potential. *Nat. Med.* **19**, 1252–1263 (2013).
28. Y. Q. Li *et al.*, Gsα deficiency in adipose tissue improves glucose metabolism and insulin sensitivity without an effect on body weight. *Proc. Natl. Acad. Sci. U.S.A.* **113**, 446–451 (2016).
29. U. M. Gundra *et al.*, Alternatively activated macrophages derived from monocytes and tissue macrophages are phenotypically and functionally distinct. *Blood* **123**, e110–e122 (2014).
30. L. Bosurgi *et al.*, Macrophage function in tissue repair and remodeling requires IL-4 or IL-13 with apoptotic cells. *Science* **356**, 1072–1076 (2017).
31. H. Qing *et al.*, Origin and function of stress-induced IL-6 in murine models. *Cell* **182**, 372–387.e14 (2020).
32. Y. Ge *et al.*, Adipokine apelin ameliorates chronic colitis in Il-10$^{-/-}$ mice by promoting intestinal lymphatic functions. *Biochem. Pharmacol.* **148**, 202–212 (2018).
33. F. Wei *et al.*, PGRN protects against colitis progression in mice in an IL-10 and TNFR2 dependent manner. *Sci. Rep.* **4**, 7023 (2014).
34. Y. Zhang, M. Brenner, W. L. Yang, P. Wang, Recombinant human MFG-E8 ameliorates colon damage in DSS- and TNBS-induced colitis in mice. *Lab. Invest.* **95**, 480–490 (2015).
35. L. Santucci *et al.*, Galectin-1 suppresses experimental colitis in mice. *Gastroenterology* **124**, 1381–1394 (2003).
36. J. Nedergaard, B. Cannon, The browning of white adipose tissue: Some burning issues. *Cell Metab.* **20**, 396–407 (2014).